

Path selection in the growth of rivers

Yossi Cohen^{a,1}, Olivier Devauchelle^b, Hansjörg F. Seybold^a, Robert S. Yi^a, Piotr Szymczak^c, and Daniel H. Rothman^a

^aLorenz Center, Department of Earth, Atmospheric and Planetary Sciences, Massachusetts Institute of Technology, Cambridge, MA 02139; ^bInstitut de Physique du Globe, 75252 Paris Cedex 05, France; and ^cInstitute of Theoretical Physics, Faculty of Physics, University of Warsaw, 02-093, Warsaw, Poland

Edited by Grigory Isaakovich Barenblatt, University of California, Berkeley, CA, and approved September 9, 2015 (received for review July 21, 2014)

River networks exhibit a complex ramified structure that has inspired decades of studies. However, an understanding of the propagation of a single stream remains elusive. Here we invoke a criterion for path selection from fracture mechanics and apply it to the growth of streams in a diffusion field. We show that, as it cuts through the landscape, a stream maintains a symmetric groundwater flow around its tip. The local flow conditions therefore determine the growth of the drainage network. We use this principle to reconstruct the history of a network and to find a growth law associated with it. Our results show that the deterministic growth of a single channel based on its local environment can be used to characterize the structure of river networks.

river channels | principle of local symmetry | harmonic growth | Loewner equation | fracture mechanics

As water flows, it erodes the land and produces a network of streams and tributaries (1–3). Each stream continues to grow with the removal of more material, and evolves in a direction that corresponds to the water flux entering its head. The prediction of the trajectory of a growing channel and the speed of its growth are important for understanding the evolution of complex patterns of channel networks. Several models address their evolution and ramified structure. One, the Optimal Channel Networks model (4), is based on the concept of energy minimization and suggests a fractal network. The landscape evolution method and many diffusion-based models (5–7) have also proven useful for modeling erosion and sediment transport. These models distinguish between two regimes: one is a diffusion-dominated regime where topographic perturbations are diminished, which leads to a smoother landscape and uniform symmetric drainage basins. In this case, the shape of a channel cannot deviate from a straight line. In the second regime, advection dominates, and channel incisions are amplified. The channel effectively continues to the next point that attracts the largest drainage basin, which corresponds to the direction where it receives the maximum water flux. These models nicely predict the formation of ridges and valleys and provide insight into the interaction between advective and diffusive processes (8, 9). However, they do not address directly the evolution of a single channel and do not explicitly address the nature of a growing stream based on its local environment.

Here we address two basic questions in the evolution and the dynamics of a growing channel: where it grows and at what velocity. We propose that, when streams are fed by groundwater, the direction of the growth of a stream is defined by the groundwater flow in the vicinity of the channel head. This theory is widely used in the framework of continuum fracture mechanics and accurately predicts crack patterns in different fracture modes, for both harmonic and biharmonic fields and for different stress singularities (10–12). The theory, known as the principle of local symmetry, states that a crack propagates along the direction where the stress distribution is symmetric with respect to the crack direction (10, 13). We find an analog of this principle in the motion and growth of channels in a diffusive field. We argue that the trajectory of a stream is dictated by the symmetry of the field in the vicinity of its head. We also demonstrate how to determine a growth law that ties the water flux into a channel to an erosion process and the propagation velocity of a channel head.

Principle of Local Symmetry

We study the case of channel growth driven by groundwater seepage as a process representative of channel formation and growth in a diffusing field (2, 14–19). The emergence of groundwater through the surface leads to erosion and the development of a drainage network (17). The flow of groundwater is described by Darcy's law (2),

$$\mathbf{v} = -\kappa \nabla \left(\frac{p}{\rho g} + z \right). \quad [1]$$

Here \mathbf{v} is the fluid velocity, κ the hydraulic conductivity, p the pressure in the fluid, ρ the fluid density, z the geometric height, and g the gravitational acceleration. By assuming only horizontal flow, the Dupuit approximation (20, 21) relates the water table height $h(x, y)$ to the groundwater horizontal velocity $\mathbf{v} = -\kappa \nabla h$, and to the groundwater flux $\mathbf{q} = -h\kappa \nabla h = -(\kappa/2) \nabla h^2$. Considering an incompressible flow, the steady-state solution for the water table height becomes a function of the ratio between the mean precipitation rate P and κ ,

$$\frac{\kappa}{2} \nabla^2 h^2 = -P. \quad [2]$$

Thus, the square of the height h is a solution of the Poisson equation (21, 22). We assume that the hydraulic conductivity κ is constant. By rescaling the field, Eq. 2 becomes

$$\nabla^2 \phi = -1, \quad [3]$$

where $\phi = (\kappa/2P)h^2$, and $-\nabla \phi$ is the Poisson flux. The boundaries are given by the stream network; for a gently sloping stream we can assume that the water table elevation at the boundary is $h = 0$, and therefore $\phi = 0$ along the streams.

Here we investigate how the groundwater flow controls the growth of a channel. In the vicinity of the channel head we can

Significance

The complex patterns of river networks evolve from interactions between growing streams. Here we show that the principle of local symmetry, a concept originating in fracture mechanics, explains the path followed by growing streams fed by groundwater. Although path selection does not by itself imply a rate of growth, we additionally show how local symmetry may be used to infer how rates of growth scale with water flux. Our methods are applicable to other problems of unstable pattern formation, such as the growth of hierarchical crack patterns and geologic fault networks, where dynamics remain poorly understood.

Author contributions: Y.C., O.D., H.F.S., and D.H.R. designed research; Y.C., O.D., R.S.Y., P.S., and D.H.R. performed research; Y.C. and D.H.R. analyzed data; and Y.C., O.D., P.S., and D.H.R. wrote the paper.

The authors declare no conflict of interest.

This article is a PNAS Direct Submission.

¹To whom correspondence should be addressed. Email: ycohen@mit.edu.

This article contains supporting information online at www.pnas.org/lookup/suppl/doi:10.1073/pnas.1413883112/-DCSupplemental.

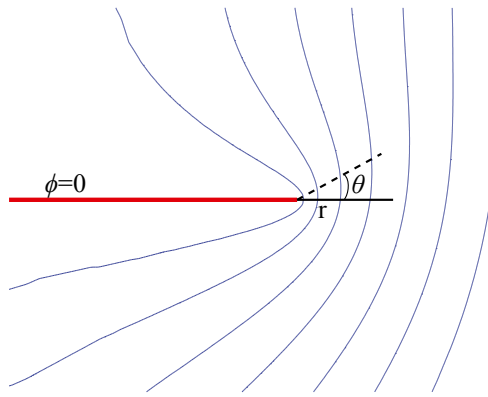


Fig. 1. Channel (in red) in a Poisson field. The equipotential lines of the field are in blue. r is the distance from the channel head, and $\theta=0$ indicates the growth direction of the channel.

neglect the Poisson term in Eq. 3, and the field can be approximated as (23, 24)

$$\nabla^2 \phi = 0. \quad [4]$$

For a semiinfinite channel on the negative x axis with boundary conditions

$$\phi(\theta = \pm\pi) = 0, \quad [5]$$

the harmonic field around the tip can be expressed in cylindrical coordinates as (23)

$$\phi(r, \theta) = a_1 r^{1/2} \cos\left(\frac{\theta}{2}\right) + a_2 r \sin(\theta) + \mathcal{O}(r^{3/2}), \quad [6]$$

where, as shown in Fig. 1, r is the distance from the channel head and the channel is located at $\theta = \pm\pi$. The coefficients a_i , $i=1,2$ are determined by the shape of the water flux coming from the outer boundary.

Because the leading term in the expansion of Eq. 6 is symmetric with respect to θ , we do not expect it to influence the direction in which the channel grows. Thus, we must consider the subdominant term that breaks the symmetry and can therefore cause the stream to bend as it grows. Other terms in the expansion are negligible in the vicinity of the channel head.

In fracture mechanics, a crack maintains a symmetric elastic field around its tip to release the maximum stress as it propagates (10, 13). Inspired by this example, we suggest that a channel grows in the direction which maintains a locally symmetric groundwater flow. Accordingly, we formulate an analog of the principle of local symmetry as follows: A channel grows in the direction for which the coefficient a_2 vanishes. Fig. 2 expresses this notion pictorially.

Evaluation of the Principle of Local Symmetry

We now evaluate the principle of local symmetry (PLS) from three points of view. First, we justify its application to channel networks based on simple physical reasoning. We then show that the PLS is mathematically equivalent to assuming that a channel grows along the groundwater flow lines, an assumption that has been shown to be consistent with field observations (24). Finally, we describe a numerical procedure to grow a network according to this principle.

Negative Feedback Induced by Groundwater. As a channel grows, it moves the boundary of the network, and this changes the groundwater flow near the tip of the channel. Mathematically,

the coefficients a_n of the expansion of the local flow field near the tip [6] vary during the channel's growth.

To understand how groundwater controls growth, we study the influence of the coefficient of the first two dominant terms (as $r \rightarrow 0$) a_1 and a_2 on the distribution of groundwater into the channel. At a distance r from the channel's head, the amount of water collected through the right-hand side of the stream reads

$$Q_{\text{right}} = \int_0^r \frac{\partial \phi}{\partial \theta} \Big|_{\theta=-\pi} \frac{dr'}{r'} \approx a_1 \sqrt{r} - a_2 r. \quad [7]$$

Similarly, the amount of water collected through the left-hand side reads

$$Q_{\text{left}} \approx a_1 \sqrt{r} + a_2 r. \quad [8]$$

For illustration, let us assume that the second coefficient a_2 is negative. Eqs. 7 and 8 indicate that more groundwater seeps into the stream through its right-hand bank ($\theta < 0$) than through its left-hand bank ($\theta > 0$). We expect this asymmetric seepage to erode the bank collecting more groundwater faster, thus causing

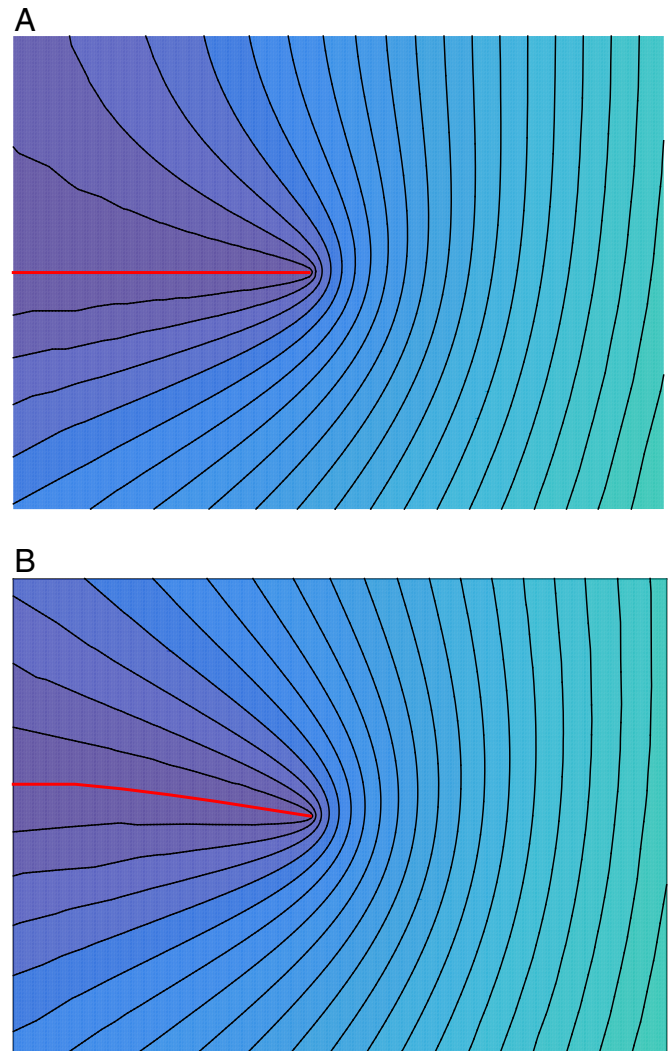


Fig. 2. (A) Asymmetric field ($a_2 \neq 0$): as the stream grows, it must bend in a direction for which a_2 vanishes. (B) Symmetric field ($a_2 = 0$): Growth according to the principle of local symmetry.

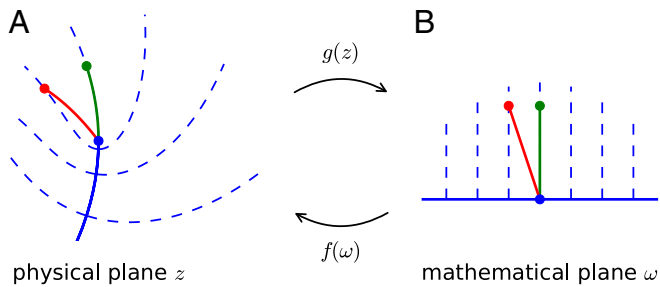


Fig. 3. Streamline growth: (A) in the physical plane, and (B) in the mathematical plane. The channel (solid blue) growing along a flow line that enters the tip is geodesic (green). Red line: example of nongeodesic growth.

the channel's head to bend toward the stronger source of water. By turning its head toward the more intense groundwater flux, the channel reduces the local asymmetry of the flow near its tip. Therefore, we hypothesize that, as a consequence of this negative feedback, a channel maintains a locally symmetric groundwater flow in the vicinity of the tip as it grows.

Equivalence with Geodesic Growth. The geometry of a network draining a diffusion field depends on the dynamics of its growth. In particular, when two nascent tips grow off of a parent channel, the angle of this bifurcation depends on the growth rule. For instance, if a channel grows along the stream line that intersects its tip (Fig. 3A), it should bifurcate at $2\pi/5 = 72^\circ$ (24). This value accords with field measurements collected in a small river network near Bristol, Florida. This observation suggests that a channel cuts its path in the surrounding landscape along the groundwater flow line. We refer to this growth rule as “geodesic growth” (25), and connect it to the PLS.

To grow numerically a network in a diffusion field, one typically needs to (i) solve the diffusion field around the network, (ii) evolve the network according to the local properties of the field near its tips, and repeat these operations (23). Whether the diffusion field satisfies the Poisson equation 3 or the Laplace equation 4 does not impact significantly the numerical procedure. However, complex analysis facilitates considerably the derivation of formal results about network growth in Laplacian fields.

In particular, the Laplacian field representing the groundwater flow defines a complex map from the physical plane to the upper

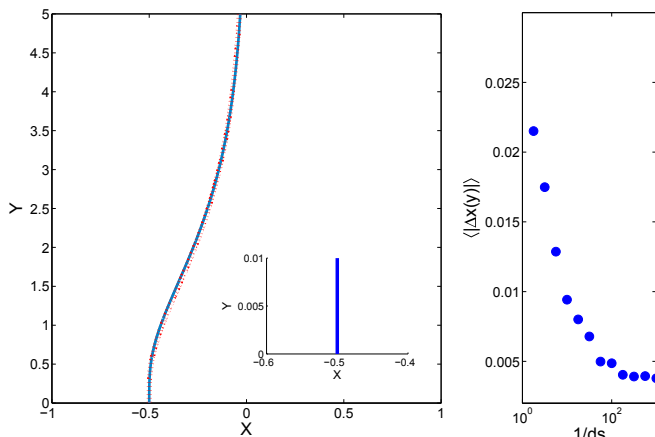


Fig. 4. (Left) Trajectory of a single stream initiated at the bottom, to the left of center. Blue: the analytical solution (28). Red: the numerical trajectory of a stream grown according to the PLS. (Inset) The initial slit. (Right) The average error $\langle |\Delta x(y)| \rangle$ between the numerical trajectory and the analytical solution with the decrease of the step size, ds .

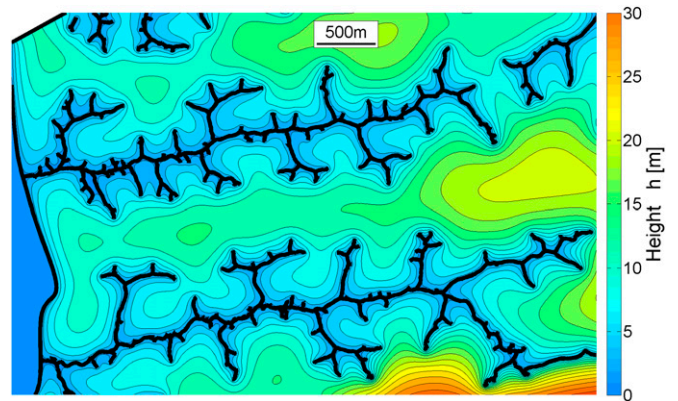


Fig. 5. Height h of the water table above a seepage network (black) in Bristol, FL. The shape of the water table is calculated using Eq. 2, assuming the channel network is an absorbing boundary at $h = 0$ and $P/\kappa = 3.125 \times 10^{-3}$ (30).

half-plane (Fig. 3). This map encapsulates both the geometry of the network at a specific time, and the groundwater flow around it. Translating geodesic growth and local symmetry into this formalism, we find that they define the same growth rule (*SI Equivalence Between Geodesic Growth and Local Symmetry*).

This equivalence does not necessarily hold when the channel grows in a field which satisfies the Poisson equation. However, because the above demonstration is based on the local properties of the field, the source term of the Poisson equation comes as an external flux only. We therefore expect that the PLS is but a reformulation of geodesic growth, which accords with field observation. An important consequence of this reformulation is the ability to specify the growth direction in a precise, well-controlled manner, to which we now turn.

Numerical Implementation. We design a numerical method to calculate trajectories that explicitly maintain local symmetry, and compare its results to an analytic solution. We consider a simple case in which one channel grows in a confined rectangular geometry $-1 < x < 1, 0 < y < 30$ in a Laplacian field. We first calculate the trajectory using the PLS. Our algorithmic implementation of this principle requires that at each step streams grow in the direction for which a_2 vanishes. (Further details are in *SI Propagation of a Channel*.) We apply the following boundary conditions: a zero elevation at the bottom ($\phi = 0$ at $y = 0$), which corresponds to a main river or an estuary; no flux at the sides ($\partial\phi/\partial x = 0$ at $x = 1, -1$), which corresponds to a groundwater divide; and a constant flux of water from the top, ($\partial\phi/\partial y = 1$). We then initiate a small slit ($l = 0.01$) perpendicular to the bottom edge, and allow it to grow according to the PLS. Not surprisingly, a stream initiated at the middle of the lower edge ($x = 0; y = 0$) continues straight. However, when we break the symmetry and initiate a slit left of the center ($x = -0.5; y = 0$) the stream bends toward the center of the box.

To validate our numerical implementation of the PLS, we compare our numerical trajectory to the evolution of a path in a Laplacian field according to the deterministic Loewner equation (26–28). In the Loewner model, the properties of analytic functions in the complex plane are used to map the geometry into the complex half-plane or into radial geometry, and to find the solution for the field. Then, at each time step, a slit is added to the tip of the channel based on the gradient of the field entering the tip. Fig. 4 compares results from the two approaches. We find that the two solutions exhibit the same trajectory.



Fig. 6. Retracted channel (blue) with two growth mechanisms: following local symmetry (red), and continuing in the tangent direction (green). The error angles β and φ are calculated between a real trajectory of a channel (dashed blue) and a trajectory that follows local symmetry, and a real trajectory and the tangent, respectively. We find that the mean absolute value of the error angle measured for 255 channels in Florida is $\langle|\beta|\rangle = 3.67 \pm 0.2$ for the local symmetry and $\langle|\varphi|\rangle = 5.62 \pm 0.2$ for the tangent direction.

Growth of a Real Stream Network

The evolution of a channel is defined by the field in the vicinity of the tip. However, this field is nonlocal and highly dependent on the boundary conditions imposed by the ramified network of the streams. In this section, the numerical method developed in the previous section is used to compute trajectories in more general settings where no analytic solutions are possible.

Growth According to Local Symmetry. We seek to determine if growth of a real stream network is consistent with the PLS. We study a network of seepage valleys located near Bristol, FL on the Florida Panhandle (17). The network is presented in Fig. 5. The valley network is obtained from a high-resolution LIDAR (Light Detection and Ranging) map with horizontal resolution of 1.2 m and vertical resolution of less than 5 cm (17). In this network, groundwater flows through unconsolidated sand above the relatively impermeable substratum, and into the streams (17, 29). Previous analyses indicate that the homogeneity of the sand is consistent with the assumption of constant κ (18, 19, 24, 30). The flow is determined by the Poisson equation 2; thus, the network grows in a Poisson field (30).

We study the evolution of this network and check if the growth of the streams fulfills local symmetry. First, we set the boundary conditions; because the change in elevation along the Florida network is small (the median slope $\sim 10^{-2}$), we approximate the height of the channels above the impermeable layer as constant and choose $\phi(h=0) = 0$. The outer boundaries are reflective, i.e., $\partial\phi/\partial n = 0$, corresponding to a groundwater divide. We calculate the Poisson field, Eq. 3, and find for each channel head the coefficient a_1 in the expansion 6 that corresponds to the water flux entering the tip. Then, we remove a segment, l_i , from the tip of the i th tributary and propagate it forward to its original length in five small steps (to reduce numerical error). The growth of each stream is characterized by two variables: its growth rate and the direction of its growth. We assume that the velocity of a stream is proportional to the magnitude of the gradient of the field, raised to a power η :

$$v \sim |\nabla\phi|^\eta \sim a_1^\eta. \quad [9]$$

A similar growth law has been considered in Laplacian path models (25, 28) and related erosion models (31–33). Thus, the length l_i of each segment that we remove from a channel, and later add as it grows forward, is defined according to its relative velocity; $l_i \propto v_i/\langle v \rangle$, where $v_i \propto a_{1i}$ of the i th channel ($\eta = 1$) and $\langle v \rangle = 1/n \sum_i v_i$ is the mean velocity. We fix the total length removed from the network of n tributaries to be n meters. Each channel then grows in a direction that fulfills local symmetry, i.e., in the direction for which a_2 vanishes. After we grow the network back to its original length, we study each of the tributaries separately, and measure the angle, β , between the real trajectory of the stream and the reconstructed trajectory. We perform this calculation for 255 channel heads in the Florida network. We obtain a mean of β around zero with an SD of $\sim 7^\circ$. Different

values of η give a similar distribution. We find that a mean around 0 of the angle error is consistent with a growth that fulfills local symmetry. However, some of the streams deviate significantly from their real growth direction, which may suggest that other factors account for their growth.

To evaluate the significance of the results, we suggest a null hypothesis in which the streams grow in the direction of the tangent regardless of the value of a_2 . We obtain the direction of the tangent based on the last two grid points (approximately 2 m) of the channel trajectory after retraction. Then, we calculate the angle, φ , between the tangent direction and the real trajectory, as shown in Fig. 6. We find that a growth according to the PLS reduces on average the error angle by 50% compared with growth in the direction of the tangent, and therefore improves prediction of future growth relative to the null model. An F test (34) shows that the reduction of the variance using PLS is statistically significant, with $P < 10^{-9}$ (assuming each measurement is statistically independent).

Growth Law. To understand the deviations between the real and the calculated path, we hypothesize that the deviant streams grew in a different environment than currently exists, e.g., the neighboring tributaries were relatively undeveloped (or overdeveloped) when the studied stream reached its current location. To illustrate this idea, in Fig. 7 we show the trajectories of two streams with different velocities, and compare their evolution in Poisson field for different growth exponents η . One notices that for smaller η the slower streams are more likely to deviate from their real trajectory, but for higher η the faster streams change their course. Only when $\eta = \eta_0$ (the correct value of η), any errors will remain uncorrelated to the velocity of the streams.

Motivated by this reasoning, we study the correlation between the flux entering the tip, which we identify with a_1 , and the angle β for different values of η . Retracting the network with different η creates different boundary conditions and influences the

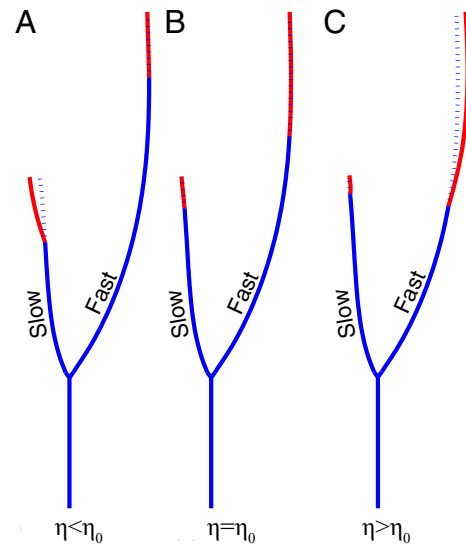


Fig. 7. Bifurcated channel (blue) is retracted with different growth exponents η ; η_0 is the exponent that characterizes the original growth. The length of the retracted segment (dashed blue) is proportional to a_1^η . The faster stream has a bigger a_1 . Thus, the segment that is removed from the faster stream becomes longer with respect to the slower stream as η gets larger. The red curves are trajectories of channels grown forward. The deviation angle β is measured between the real (dashed blue) and calculated (red) trajectories. In A, deviations are characterized by growth away from the fast stream; in C, the deviant growth avoids the slow streams; only in B, when $\eta = \eta_0$, deviations are not correlated to the velocity of the streams.

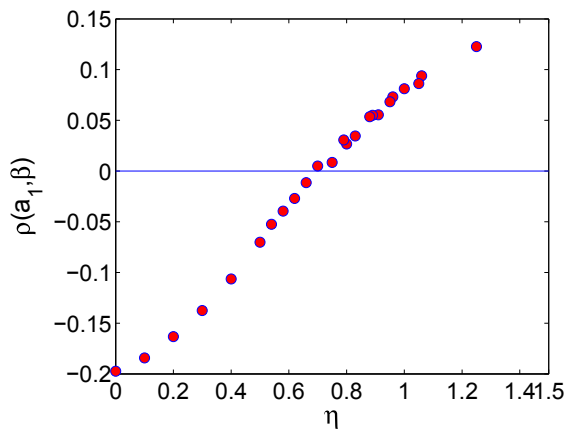


Fig. 8. Spearman rank correlation function $\rho(a_1, \beta)$ for different η between a_1 , the flux entering the tip of a channel, and β , the angle between the real trajectory of a stream and the calculated trajectory. The change in sign near $\eta = 0.7$ suggests that the Florida network grew with an exponent $\eta \approx 0.7$.

trajectory of the streams as they grow forward. For small $\eta < \eta_0$, the dependence of the length on the flux becomes weaker. In particular, when $\eta = 0$, this dependence vanishes and the same segment size is removed from each stream (Fig. 7A). Thus, as we grow the network forward, the deviation from the real trajectory will be larger for the slower streams, with small a_1 , because they try to avoid the faster streams that currently exist in their environment. However, when $\eta > \eta_0$, the faster streams are retracted much further backward compared with slower streams, and they grow in a more developed network than the network that had existed when they had actually grown in the field. In this case, the faster streams will reveal a bigger error in their trajectory. For $\eta = \eta_0$, there is no correlation between the flux and β , which suggests that η_0 is the best exponent for the growth. Fig. 8 shows that $\eta_0 \approx 0.7$ for the Florida network.

The importance of the growth exponent η is in the evolution of the network: Negative η will generate a stable network in which each perturbation, or small channel, will survive regardless of the water flux entering the tip. A positive η results in an unstable structure in which a small difference in the velocity of two

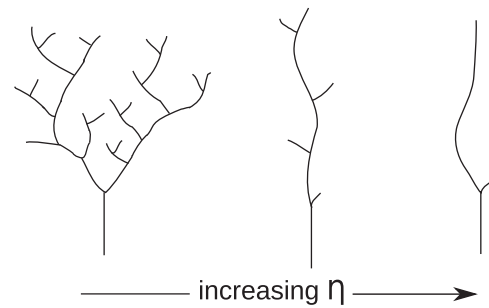


Fig. 9. Illustration of the ramified structure for increasing growth exponent η .

competing channels is amplified and may lead to a screening mechanism and the survival only of the faster channel (28). Fig. 9 contains a schematic representation of this concept. The small positive exponent found for the stream network in Florida indicates that this network is unstable. This conclusion is consistent with the prediction of a highly ramified network.

Summary

In summary, we offer a criterion for path selection of a stream in a diffusing field. We show that this criterion, which is based on the PLS (10, 13), predicts accurately the evolution of channels fed by groundwater. We suggest a method to infer the history of a real network by reconstructing it according to the PLS and evaluating errors for different growth laws. We parameterize the large-scale relationship between water flux and sediment transport with a single exponent and show that for the Florida network this growth exponent is roughly 0.7. We envision that our methods may also be applied to other problems, such as the growth of hierarchical crack patterns (35–37) and geological fault networks (38), to provide a better understanding of their evolution.

ACKNOWLEDGMENTS. Inspiration for this work derived in part from visits to the Apalachicola Bluffs and Ravines Preserve. We thank D. Printiss and The Nature Conservancy for access to the Preserve. This work was supported by Department of Energy Grant FG02-99ER15004. P.S. acknowledges the support by the National Science Centre (Poland) under Research Grant 2012/07/E/ST3/01734.

- Horton R E (1945) Erosional development of streams and their drainage basins; hydrophysical approach to quantitative morphology. *Geol Soc Am Bull* 56(3):275–370.
- Dunne T (1980) Formation and controls of channel networks. *Prog Phys Geogr* 4(2): 211–239.
- Rodríguez-Iturbe I, Rinaldo A (2001) *Fractal River Basins: Chance and Self-Organization* (Cambridge Univ Press, Cambridge, UK).
- Maritan A, Colaioni F, Flammini A, Cieplak M, Banavar JR (1996) Universality classes of optimal channel networks. *Science* 272(5264):984–986.
- Tucker GE, Bras RL (1998) Hillslope processes, drainage density, and landscape morphology. *Water Resour Res* 34(10):2751–2764.
- Fernandes NF, Dietrich WE (1997) Hillslope evolution by diffusive processes: The timescale for equilibrium adjustments. *Water Resour Res* 33(6):1307–1318.
- Perron JT, Kirchner JW, Dietrich WE (2009) Formation of evenly spaced ridges and valleys. *Nature* 460(7254):502–505.
- Smith TR, Bretherton FP (1972) Stability and the conservation of mass in drainage basin evolution. *Water Resour Res* 8(6):1506–1529.
- Perron JT, Dietrich WE, Kirchner JW (2008) Controls on the spacing of first-order valleys. *J Geophys Res* 113(F4):F04016.
- Barenblatt GI, Cherepanov GP (1961) On brittle cracks under longitudinal shear. *J Appl Math Mech* 25(6):1654–1666.
- Goldstein RV, Salganik RL (1974) Brittle-fracture of solids with arbitrary cracks. *Int J Fract* 10(4):507–523.
- Cohen Y, Procaccia I (2010) Dynamics of cracks in torn thin sheets. *Phys Rev E Stat Nonlin Soft Matter Phys* 81(6 Pt 2):066103.
- Cotterell B, Rice JR (1980) Slightly curved or kinked cracks. *Int J Fract* 16(2):155–169.
- Dunne T (1969) Runoff production in a humid area. PhD thesis (Johns Hopkins University, Baltimore).
- Dunne T (1990) Hydrology, mechanics, and geomorphic implications of erosion by subsurface flow. *Spec Pap Geol Soc Am* 252:1–28.
- Dietrich WE, Dunne, T (1993) The channel head. *Channel Network Hydrology*, eds Beven K, Kirkby MJ (John Wiley and Sons, Chichester, UK), pp 175–219.
- Abrams DM, Lobkovsky AE, Petroff AP, Straub KM, McElroy B, Mohrig DC, Kudrolli A, Rothman DH (2009) Growth laws for channel networks incised by groundwater flow. *Nat Geosci* 2(3):193–196.
- Devauchelle O, Petroff AP, Lobkovsky AE, Rothman DH (2011) Longitudinal profile of channels cut by springs. *J Fluid Mech* 667:38–47.
- Petroff AP, Devauchelle O, Kudrolli A, Rothman DH (2012) Four remarks on the growth of channel networks. *C R Geosci* 344(1):33–40.
- Bear J (1972) *Dynamics of Fluids in Porous Media* (Elsevier, New York).
- Dupuit J (1863) *Études théoriques et pratiques sur le mouvement des eaux dans les canaux découverts et à travers les terrains perméables* (Dunod, Paris), 2nd Ed.
- Polubarinova-Kochina PY (1962) *Theory of Ground Water Movement* (Princeton Univ Press, Princeton).
- Petroff AP, Devauchelle O, Seybold H, Rothman DH (2013) Bifurcation dynamics of natural drainage networks. *Philos Trans R Soc, A* 371(2004):20120365.
- Devauchelle O, Petroff AP, Seybold HF, Rothman DH (2012) Ramification of stream networks. *Proc Natl Acad Sci USA* 109(51):20832–20836.
- Carleson L, Makarov N (2002) Laplacian path models. *J Anal Math* 87(1):103–150.
- Löwner K (1923) Untersuchungen über schlichte konforme Abbildungen des Einheitskreises. I. *Math Ann* 89(1):103–121.
- Gruzberg IA, Kadanoff LP (2004) The Loewner equation: Maps and shapes. *J Stat Phys* 114(5-6):1183–1198.
- Gubiec T, Szymczak P (2008) Fingered growth in channel geometry: A Loewner-equation approach. *Phys Rev E Stat Nonlin Soft Matter Phys* 77(4 Pt 1):041602.
- Schumm SA, Boyd KF, Wolff CG, Spitz WJ (1995) A ground-water sapping landscape in the florida panhandle. *Geomorphology* 12(4):281–297.
- Petroff AP, Devauchelle O, Abrams DM, Lobkovsky AE, Kudrolli A, Rothman DH (2011) Geometry of valley growth. *J Fluid Mech* 673:245–254.
- Howard AD, Kerby G (1983) Channel changes in badlands. *Geol Soc Am Bull* 94:739–752.

32. Stock JD, Montgomery DR (1999) Geologic constraints on bedrock river incision using the stream power law. *J Geophys Res: Solid Earth* 104(B3):4983–4993.
33. Whipple KX, Tucker GE (1999) Dynamics of the stream-power river incision model: Implications for height limits of mountain ranges, landscape response timescales, and research needs. *J Geophys Res: Solid Earth* 104(B8):17661–17674.
34. Press WH (2007) *Numerical Recipes, 3rd Edition: The Art of Scientific Computing* (Cambridge Univ Press, Cambridge, UK).
35. Skjeltorp AT, Meakin, P (1988) Fracture in microsphere monolayers studied by experiment and computer simulation. *Nature* 335(6189):424–426.
36. Bohn S, Platkiewicz J, Andreotti B, Adda-Bedia M, Couder Y (2005) Hierarchical crack pattern as formed by successive domain divisions. II. From disordered to deterministic behavior. *Phys Rev E Stat Nonlin Soft Matter Phys* 71(4 Pt 2):046215.
37. Cohen Y, Mathiesen J, Procaccia I (2009) Drying patterns: Sensitivity to residual stresses. *Phys Rev E Stat Nonlin Soft Matter Phys* 79(4 Pt 2):046109.
38. Dolan JF, Bowman DD, Sammis CG (2007). Long-range and long-term fault interactions in southern california. *Geology* 35(9):855–858.
39. Kwon YW, Bang H (2000) *The Finite Element Method Using MATLAB* (CRC, Boca Raton, FL).

Supporting Information

Cohen et al. 10.1073/pnas.1413883112

SI Equivalence Between Geodesic Growth and Local Symmetry

Here we propose a detailed version of the reasoning briefly exposed in the main text. We first formulate the growth of a channel in a Laplacian field as the evolution of a conformal map, through the Loewner equation. We then establish the equivalence between geodesic growth and local symmetry in this framework.

Conformal Map. The diffusive field which surrounds the network satisfies Laplace's equation. It is therefore the imaginary part of an analytical function $g_t \equiv g(t, z)$, where the complex variable $z = x + iy$ and $t =$ time. The imaginary part of g_t vanishes on the network due to the boundary conditions, Eq. 5. By construction, the imaginary part of g_t represents the diffusive field in Eq. 4 at time t ,

$$\phi = \text{Im}(g_t), \quad [\text{S1}]$$

and it vanishes on the channels. We take $g_t(z) \rightarrow z$ at infinity. The function g_t defines a conformal map between the physical space and the upper half-plane (main text, Fig. 3). This map unfolds the network onto the real axis and, similarly, unfolds every contour line of the diffusive field onto a horizontal line. It therefore encapsulates both the network geometry and the diffusive field around it. Based on this property, Loewner proposed to describe the domain deformation through an evolution equation for the map itself (26, 27).

Loewner Equation. Following Loewner, we decompose the growth of a channel into a series of infinitesimal slit maps, each of which further increments the length of the channel (Fig. S1) (28).

Setting the length of each increment to zero, the continuous equation describing the growth of N channels in the physical plane reads (28)

$$\dot{g}_t = \sum_{n=1}^N \frac{d_n}{g_t - p_n}, \quad [\text{S2}]$$

where d_n and $p_n(t)$ are real growth factors and the positions of the poles, respectively, at time t for the n th channel in the mathematical plane. Note that the poles are the position of the tips in the mathematical plane. The growth factor sets the velocity at which a tip grows, whereas the motion of the pole sets the direction of its growth.

We define the inverse map $f_t \equiv f(t, w)$ such as

$$f_t \circ g_t(z) \equiv f_t(g_t(z)) = z. \quad [\text{S3}]$$

Differentiation of Eq. S3 with respect to t defines the evolution of the inverse map as

$$\dot{f}_t = \frac{f'_t}{\varphi}, \quad [\text{S4}]$$

where \bullet' and $\dot{\bullet}$ denote the derivation with respect to w and t , respectively. $\varphi(w)$ is defined by

$$\frac{1}{\varphi} = -\dot{g}_t = -\sum_{n=1}^N \frac{d_n}{\omega - p_n}, \quad [\text{S5}]$$

and is an analytical function in the upper half-plane which embodies the growth of the network. Its imaginary part vanishes on the real axis, and each pole p_n is a root of it.

The motion of the poles p_n in the mathematical plane determines how the network grows in the physical plane. To establish the equivalence between geodesic growth and the PLS, we need to understand how these two rules move the poles in the mathematical plane.

Geodesic Growth. By definition, geodesic growth means that the channel's tip at time $t + \delta t$ belongs to the stream line intersecting the tip at time t , i.e., $g(\gamma_{t+\delta t}) = p + i\delta l$. Here $p(t)$ is the position of a tip in the mathematical plane at time t , and δl is a real number which defines the extension of the channel during δt (Fig. S1). This gives

$$\text{Re}(g(\gamma_{t+\delta t})) \sim p, \quad [\text{S6}]$$

where $\gamma_{t+\delta t}$ is the position of the tip in the physical plane at time $t + \delta t$. The map g_t is singular in γ_t . However, we may expand it to first order in time, and apply it to $\gamma_{t+\delta t}$:

$$\text{Re}(\dot{g}_t(\gamma_{t+\delta t})) \sim \dot{p}. \quad [\text{S7}]$$

From the definition of φ , Eq. S5, we find that geodesic growth implies

$$\dot{p} \sim -\text{Re}\left(\frac{1}{\varphi(p + i\delta l)}\right). \quad [\text{S8}]$$

Expanding the Loewner function φ to second order near the pole [note that $\varphi(p) = 0$] and injecting this expansion into Eq. S8, we find, at leading order in δl (green line in Fig. 3),

$$\frac{\partial p}{\partial t} = \frac{\varphi''(p)}{2\varphi'(p)^2}. \quad [\text{S9}]$$

This equation defines mathematically the notion of geodesic growth.

PLS. Local symmetry in the physical plane means that $a_2 = 0$. Here we find an analogy to this definition in the mathematical plane. The expansion of the map g up to the first order near the tip's position γ becomes

$$g(z) = p + \hat{a}_1 \sqrt{z - \gamma} + \hat{a}_2 (z - \gamma) + \dots \quad [\text{S10}]$$

By construction of the complex field g , Eq. S1, the coefficient \hat{a}_n is consistent with the coefficient in Eq. 6, such that $a_n = |\hat{a}_n|$. The expansion of the inverse map f up to the third order in the vicinity of the pole p becomes

$$f(w) = \gamma + c_2(\omega - p)^2 + c_3(\omega - p)^3 + \dots, \quad [\text{S11}]$$

where $c_2 = f''(p)/2$ and $c_3 = f'''(p)/6$. Note that the second term in the expansion $f'(p)$ vanishes because this point is an extremum of the function.

Substitute the two expansions S10 and S11 in Eq. S3, and we find the relationship between the physical coefficients \hat{a} and the mathematical coefficients c . In particular, we find

$$c_2 = \frac{1}{\hat{a}_1^2} \quad \text{and} \quad c_3 = \frac{2 \hat{a}_2}{\hat{a}_1^4}. \quad [\text{S12}]$$

Therefore, the local symmetry is obtained in the mathematical plane when $c_3 = 0$.

Finally, applying the expansion **S11** into the Loewner equation **S4** for a single pole ($n=1$) and equating the coefficients of the $(w-p)$ up to a second order, we find

$$2 c_2 = \varphi'(p) \dot{\gamma} \quad [\text{S13}]$$

and

$$c_3 = \frac{1}{3} \frac{\partial \gamma}{\partial t} \left(\frac{\varphi''(p)}{2} - \frac{\partial p}{\partial t} \varphi'(p)^2 \right). \quad [\text{S14}]$$

The first relation simply indicates that the Loewner function φ controls the growth velocity. Eq. **S14** establishes that whenever a tip grows ($\partial \gamma / \partial t \neq 0$), the PLS ($c_3 = 0$) is equivalent to geodesic growth (Eq. **S9**).

SI Propagation of a Channel

The evolution of a channel is defined by the field in its vicinity. To find the direction in which a channel tip evolves, we developed a numerical solver using Galerkin finite element discretization on a triangular grid (39), and solved the Poisson equation, Eq. **3**, or the Laplace equation, Eq. **4**, with the described boundary conditions. Then we iteratively add a small segment to a stream in different directions (Fig. **S2**). We obtain the field by using the numerical solver, and from the field of the vicinity of the studied stream, we find the coefficients of the expansion **6**. We accept the growth in the direction where the asymmetric coefficient becomes zero, $a_2 \sim 0$.

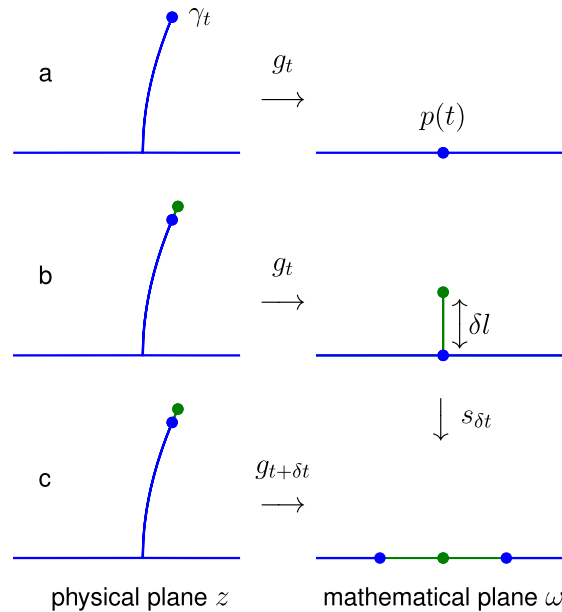


Fig. S1. Growth of a river in a Laplacian field, and evolution of the associated complex map g_t . (Left) Physical plane, (Right) mathematical plane. The map g_t maps the network at time t on the real axis (A, blue line). The slit map $s_{\delta t}$ generates a small slit in the mathematical plane, which corresponds to an infinitesimal growth of the river (B, green line). Finally, the map at time $t + \delta t$ results from the composition of the two: $g_{t+\delta t} = s_{\delta t} \circ g_t$ (C).

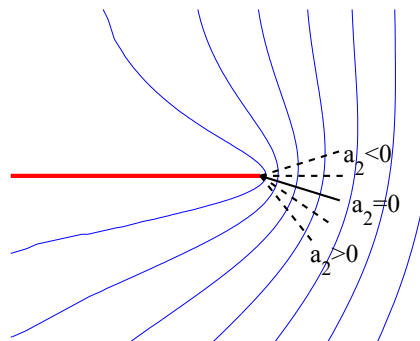


Fig. S2. Several growth directions; a channel grows in a direction in which a_2 vanishes (solid black line).